Measuring and using non-Markovianity

Carlos Pineda,[1,*] Thomas Gorin,[2] David Davalos,[1] Diego A. Wisniacki,[3] and Ignacio García-Mata[4,5]
[1]*Instituto de Física, Universidad Nacional Autónoma de México, México, D.F., 01000, México*
[2]*Departamento de Física, Universidad de Guadalajara, Guadalajara, 44840 Jalísco, México*
[3]*Departamento de Física "J. J. Giambiagi" and IFIBA, FCEyN, Universidad de Buenos Aires, 1428 Buenos Aires, Argentina*
[4]*Instituto de Investigaciones Físicas de Mar del Plata (IFIMAR), CONICET-UNMdP, B7602AYL Mar del Plata, Argentina*
[5]*Consejo Nacional de Investigaciones Científicas y Tecnológicas (CONICET), C1425FQB Argentina*
(Received 18 May 2015; published 24 February 2016)

We construct measures for the non-Markovianity of quantum evolution with a physically meaningful interpretation. We first provide a general setting in the framework of channel capacities and propose two families of meaningful quantitative measures, based on the largest revival of a channel capacity, avoiding some drawbacks of other non-Markovianity measures. We relate the proposed measures to the task of information screening. This shows that the non-Markovianity of a quantum process may be used as a resource. Under these considerations, we analyze two paradigmatic examples, a qubit in a quantum environment with classically mixed dynamics and the Jaynes-Cummings model.

DOI: 10.1103/PhysRevA.93.022117

I. INTRODUCTION

The field of open quantum systems is of paramount importance in quantum theory [1]. It helps us to understand fundamental problems such as decoherence, the quantum-to-classical transition, and the measurement problem [2]. Besides, it has been essential for reaching an impressive level of control in experiments on different quantum systems, which are the cornerstone of recent developments in quantum technologies [3–7].

The usual approach to quantum open systems relies on the assumption that the evolution has negligible memory effects. This supposition is part of the so-called Born-Markov approximation, which also assumes weak system-environment coupling and a large environment. The keystone of Markovian quantum dynamics is the Lindblad master equation [8,9], which describes the generator of quantum dynamical semigroups. The behavior of several interesting and realistic quantum systems has been studied using the Born-Markov approximation. However, these assumptions (weak coupling and large size of the environment) cannot be applied in many situations, including recent experiments of quantum control. This shows the importance of understanding quantum open systems beyond the Born-Markov approximation. A whole new area of research, under the name of quantum non-Markovianity (NM), has emerged, which includes deviations from the semigroup property, along with wider criteria.

A great amount of work (see [10–12] and references therein) has been done to understand and characterize non-Markovian quantum evolutions—or non-Markovianity, as it is generically called. This not only gives us a better understanding of open quantum systems but also provides more efficient ways to control quantum systems. For example, it was recently shown that NM is an essential resource in some instances of steady-state entanglement preparation [13,14] or can be exploited to carry out quantum control tasks that could not be realized in closed systems [15]. Besides, non-Markovian environments can speed up quantum evolutions reducing the quantum speed limit [16].

Unlike other properties, such as entanglement, there is not a unique definition of NM. There exist different criteria, more or less physically motivated, which in turn can be associated with a measure [10–12]. The two most popular criteria are based on distinguishability [17] and divisibility [18], from which two corresponding measures can be derived. There exist other measures [19–23], which basically are variations of these two or are very similar. All of these measures present some of the following problems: they lack a clear and intuitive physical interpretation, they can diverge in very generic cases [24], and they are not directly comparable to each other. Another problem is that, even if at least one of them has an intuitive physical interpretation, in terms of information flow [17], neither, to our knowledge, has a direct relation to a resource associated with a task—like entanglement of formation has.

In this work, we pursue two goals. First, we want to construct NM measures without the mentioned drawbacks. We undertake this task within the framework of channel capacities. The proposed measures are based on the maximum revival of the capacities, a characteristic that has a very simple physical interpretation and has a natural time-independent bound. Of course there might—and most likely will—exist many possible measures of quantum NM. Thus, we first provide a general setting and then put forward two plausible, meaningful quantitative measures. Our second goal is to outline the theoretical bases for considering NM as a resource.

Consider what we call a quantum vault (QV). Alice shall deposit information, classical or quantum, in a quantum physical system (say, in a physical realization of a qubit); for some period of time, during which the system evolves, the physical system can be subject to an attack by an eavesdropper, Eve; finally, after that time interval, the information is to be retrieved by Alice from the same physical system. Of course, the system interacts with an environment, which neither Alice nor Eve can access. Note that this task can be related to quantum data hiding [25–27]. We show that one of the NM measures proposed is closely related to the efficiency of the

*carlospgmat03@gmail.com

QV. Therefore the value of the measure can be considered a resource associated with a specific task.

To illustrate our ideas we analyze two examples of physical systems coupled to non-Markovian environments and analyze the newly defined measures as well as their QV capabilities. We also explain possible advantages with respect to other NM measures. First, we study a qubit, coupled via pure dephasing to an environment whose dynamics are given by a mixed quantum map. Different kinds of dynamics can be explored, changing the initial state of the environment. For the measures proposed in previous works, this sometimes leads to unexpected behavior. The other example we consider is the well-known Jaynes-Cummings model (JCM) [28], a two-level atom coupled to a bosonic bath, where we contrast our proposals with some of the most used NM measures.

The work is organized as follows. In Sec. II we describe the general framework that relates NM to the capacities of a quantum channel. Then we define two NM measures based on the largest revival of the capacities. In Sec. III we introduce the concept of the QV and show its relation to the new NM measures. Section IV is devoted to analyzing two examples using the ideas presented in the previous sections. We end the paper with some final remarks in Sec. V.

II. NON-MARKOVIANITY MEASURED BY THE LARGEST REVIVAL

The two most widespread NM measures are the one due to Breuer, Laine, and Piilo (BLP) [17], based on distinguishability (henceforth abbreviated $\mathcal{M}^{\mathrm{BLP}}$), and the one due to Rivas, Huelga, and Plenio (RHP) [18], based on divisibility ($\mathcal{M}^{\mathrm{RHP}}$). At the heart of both measures, there is a well-defined concept which has been borrowed from classical stochastic systems. In the case of $\mathcal{M}^{\mathrm{BLP}}$, it is the contraction of the probability space under Markovian stochastic processes, while in the case of $\mathcal{M}^{\mathrm{RHP}}$, it is the divisibility of the process itself. Both concepts can be used as *criteria* for quantum Markovianity by *defining* that a quantum process is Markovian if the distinguishability between all pairs of evolving states is nonincreasing ($\mathcal{M}^{\mathrm{BLP}}=0$) or if the process is divisible ($\mathcal{M}^{\mathrm{RHP}}=0$); otherwise, the process is called non-Markovian. It has been shown in Ref. [11] that the semigroup property of a quantum process implies that $\mathcal{M}^{\mathrm{RHP}}=0$ and that, if the system is Markovian according to the RHP criterion, it is also Markovian under the BLP criterion. In order to obtain the measures, both groups of authors apply essentially the same procedure: integrate a differential measure for the violation of the corresponding criterion. The same construction principle has been used in Ref. [23] to quantify NM based on channel capacities.

Consider the convex space of all quantum channels and, in this space, a continuous curve Λ_t with $0\leqslant t\leqslant\infty$ starting at the identity $\Lambda_0=\mathbb{1}$. We call such a curve a *quantum process*. Any resource $\mathcal{K}$ of interest will be a function of the space of quantum channels. Thus any quantum process comes along with the function

$$K(t)=\mathcal{K}(\Lambda_t), \tag{1}$$

quantifying the resource the quantum channel provides at time t. Postulating that $K(t)$ cannot increase during Markovian dynamics, one defines the function

$$\mathcal{M}^{\infty}_{\mathcal{K}}[\Lambda_t]=\int_{\dot{K}>0}\dot{K}(\tau)\,\mathrm{d}\tau \tag{2}$$

as a measure of NM. We use the subscript ∞ for this class of measures, as it is possible that one has to add an infinite number of contributions (all intervals where $\dot{K}>0$). We use brackets to indicate a functional in the space of quantum processes and parentheses when we refer to a functional in the space of quantum channels. One can immediately derive a criterion for NM, namely, $\mathcal{M}^{\infty}_{\mathcal{K}}[\Lambda_t]>0$. In the case of RHP,

$$\dot{K}(\tau)=\lim_{\varepsilon\to 0^{+}}\frac{\mathrm{tr}|C_{\tau+\varepsilon,\tau}|-1}{\varepsilon}, \tag{3}$$

where $\mathrm{tr}|\hat{A}|$ is the trace-norm and $C_{\tau+\varepsilon,\tau}$ is proportional to the Choi representation [29,30] of the map $\Lambda_{\tau+\varepsilon}\circ\Lambda_{\tau}^{-1}$, which evolves states from time τ to time $\tau+\varepsilon$. In the case of BLP

$$K(t)=D[\Lambda_t(\rho_1),\Lambda_t(\rho_2)], \tag{4}$$

where $D(\varrho_1,\varrho_2)=\mathrm{tr}|\varrho_1-\varrho_2|/2$ is the trace distance between the two states ϱ_1 and ϱ_2. The initial states ρ_1,ρ_2 are chosen to maximize the NM measure. The measures defined in Ref. [23] can also be cast in this form. In that case, $K(t)$ is directly defined as the corresponding channel capacity of Λ_t.

For definitiveness, two channel capacities are considered in this work: that for entanglement-assisted communication and that for quantum communication [31]. Note that also much simpler measures, such as the average fidelity, the purity, and some measure of entanglement, may be cast in that form.

This construction, which includes contributions from a possibly infinite number of intervals where $\dot{K}>0$, may result in rather inconvenient properties. The main problem stems from the overvaluation of fluctuations. Fluctuations arising from a finite-size environment, or from finite (numerical or experimental) statistics, will lead to a linear increase in the measure. This contribution will be proportional to both the time interval considered and the amplitude of the fluctuations. One must thus truncate the integration interval and smear functions or remove these contributions in another way. From a mathematical point of view, consider adding a small fluctuating term with a high frequency in a fixed interval. This will add to the measure a term proportional to the amplitude, the interval length, and the frequency. This in turn implies that neighbor functions, under any p-norm, may have arbitrarily different measures of NM under $\mathcal{M}^{\infty}_{\mathcal{K}}[\Lambda_t]$ and even diverge (a detailed example is presented in Sec. IV A, where the different measures are compared). The divergence can be remedied by normalization such as in [18], where the authors consider $\mathcal{M}^{\infty}_{\mathcal{K}}[\Lambda_t](a+\mathcal{M}^{\infty}_{\mathcal{K}}[\Lambda_t])^{-1}$ with $a=1$. However, this normalization is completely arbitrary, as any other scale for a would be equally acceptable. Even if the measures yield finite values, it is not clear how one should interpret a statement that one process has a larger value for BLP NM (RHP NM) than another. It is even less possible to compare values obtained for different measures.

Here, we show that a rather simple modification of the construction can avoid these issues and lead to a clear physical interpretation of the resulting NM measures. The modification consists of considering only the largest revival with respect to

either (i) the minimum value of $K(\tau)$ prior to the revival or (ii) the average value prior to the revival. Thus, we take

$$\mathcal{M}_{\mathcal{K}}^{\max}[\Lambda_t] = \max_{t_f,\tau\leqslant t_f}[K(t_f) - K(\tau)] \tag{5}$$

in the first case and

$$\mathcal{M}_{\mathcal{K}}^{\langle\cdot\rangle}[\Lambda_t] = \max\left\{0, \max_{t_f}\left[K(t_f) - \langle K(\tau)\rangle_{\tau<t_f}\right]\right\} \tag{6}$$

in the second. Here, $\langle\cdot\rangle_{\tau<t_f}$ denotes the time average until t_f. In the first case, we are measuring the biggest revival during the time interval, whereas in the second, we are measuring a revival, but with respect to the average behavior prior to this time. Note that

$$\mathcal{M}_{\mathcal{K}}^{\langle\cdot\rangle}[\Lambda_t] \leqslant \mathcal{M}_{\mathcal{K}}^{\max}[\Lambda_t] \tag{7}$$

as $\langle K(\Lambda_\tau)\rangle_{\tau<\tau_{\max}} \geqslant \min_{\tau<\tau_{\max}} K(\Lambda_\tau)$. Moreover, also note that

$$\mathcal{M}_{\mathcal{K}}^{\infty}[\Lambda_t] > 0 \iff \mathcal{M}_{\mathcal{K}}^{\max}[\Lambda_t] > 0, \tag{8}$$

though no such relation is found for $\mathcal{M}_{\mathcal{K}}^{\langle\cdot\rangle}$. In fact, we see later that nonmonotonic behavior *does not* guarantee a positive value for $\mathcal{M}_{\mathcal{K}}^{\langle\cdot\rangle}$.

Note that one could also take additional disjoint contributions in Eq. (5), i.e., include more nonoverlapping segments in which $\dot{K} > 0$. In this case, relations (7) and (8) would still hold, though the simple geometric interpretation of the "largest overall revival" would break. We prefer Eq. (5) for simplicity.

III. NON-MARKOVIANITY AS A RESOURCE: THE QUANTUM VAULT

We consider a quantum system which is used to store and retrieve information by state preparation and measurement. The quantum system is coupled to an inaccessible environment and we describe its dynamics by a quantum process. In order to use the system, Alice encodes her information (which may be quantum or classical) in a quantum state. Then at some later time Alice attempts to retrieves the information from the evolved quantum state. Note that this state need not be equal to the initial state; it is sufficient that Alice is able to recover her information from it. The capacity of the device depends on the amount of information which can be stored and faithfully retrieved. During the time in which the information is stored, it might be subject to an attack by an eavesdropper, Eve. Some important remarks should be made. Eve has a finite probability of attacking, and her attack destroys the quantum state. We assume that Alice becomes aware if there is an attack and discards the state. A good QV is such that Alice can obtain her information with a high reliability and, between state preparation and readout, the information is difficult to retrieve.

The process, until the measurement by Alice or Eve, is described by the quantum process Λ_τ, while the information is quantified by a capacity $\mathcal{K}$. We thus have a time-dependent value of the capacity, analogous to Eq. (1). The times considered are in the range $0 \leqslant \tau \leqslant t_f$, with t_f being the time at which Alice attempts to retrieve the information. The average information that can be obtained by Eve per attack is then $\langle K\rangle$, where the average is taken during the vault operation, namely, from 0 until t_f. Here we assume that when Eve attacks, she does so only once, as an attack destroys the state anyway. If Eve attacks with a probability q, on average she will obtain the information $q\langle K\rangle$. Thus, the average information successfully retrieved by Alice will be only $(1-q)K(t_f)$. We consider as a figure of merit the difference between the average information obtained by Alice and that obtained by Eve:

$$\Delta K_q = (1-q)K(t_f) - q\langle K\rangle. \tag{9}$$

Note that to obtain Eq. (9) the presence of an eavesdropper is crucial. It is responsible for the second term, and without it, we would have simply an equation stating how a channel capacity decays over time. Note that this quantity can be negative, when Eve obtains on average more information than Alice can retrieve. Finally, we may define the QV efficiency as $\eta_q = \Delta K_q/K_{\max}$, with $K_{\max} = \mathcal{K}(\mathbb{1})$. A good QV should have an efficiency close to 1.

Assume that $\mathcal{K}$ is normalized in such a way that $p = K/K_{\max}$ is the probability that the message encoded in the state will be retrieved. A successful run can be defined as a run in which, if Eve attacks, she gains no information, whereas if Eve does not attack, Alice retrieves the information successfully. From the considerations above, one can see that the probability of having a successful run is given by

$$P_q = q(1 - \langle p(t)\rangle) + (1-q)p(t_f) = \eta_q + q. \tag{10}$$

We associate with this probability a quality factor for the channel, as a QV, that is simply the above probability weighted by the capacity of the channel, that is, $\mathcal{N}_q = K_{\max}P_q = \Delta K_q + qK_{\max}$.

Now we discuss ΔK_q and $\mathcal{N}_q$ for some particular examples and establish its relation to $\mathcal{M}_{\mathcal{K}}^{\langle\cdot\rangle}$. We first examine the worst-case scenario: $q \approx 1$. By definition, if Eve attacks, she destroys the state. This fact is reflected in ΔK_q, which can go from the minimal value $-K_{\max}$ (worst efficiency; η_q) to $\Delta K_q = 0$ (poor QV) when $\langle K(t)\rangle \approx 0$. $\mathcal{N}_q$, on the other hand, ranges from $\mathcal{N}_q = 0$ (i.e., bad QV) to $\mathcal{N}_q = K_{\max}$. In the latter case a large $\mathcal{N}_q$ value due to a small $\langle K(t)\rangle$ evidences the fact that Eve is unable to obtain anything. In the best-case scenario of $q \ll 1$, evidently the efficiency of the vault is only tied to $K(t_f)$, the larger the better.

Now let us assess the general case. We only take into account the case where $\mathcal{M}^{\langle\cdot\rangle} > 0$, i.e., from Eq. (6) there is at least one t_f for which $\langle K(t)\rangle < K(t_f)$. The first relation between the QV and $\mathcal{M}_{\mathcal{K}}^{\langle\cdot\rangle}$ that we find is

$$\min(1-q,q)\times\mathcal{M}_{\mathcal{K}}^{\langle\cdot\rangle} \leqslant \Delta K_q \leqslant \max(1-q,q)\times\mathcal{M}_{\mathcal{K}}^{\langle\cdot\rangle}, \tag{11}$$

which is easy to derive from the definition, provided t_f is the same for both. This relation sets lower and upper bounds for the QV, depending on q and $\mathcal{M}^{\langle\cdot\rangle}$ [a corresponding relation with $\mathcal{N}_q$ follows directly from Eq. (10)]. If there is no information about the attack probability, and assuming that all probabilities are uniformly likely, we can assume, invoking a maximum entropy principle, an average probability of $q = 1/2$. For this unbiased case (and $\mathcal{M}^{\langle\cdot\rangle} > 0$) we have

$$\Delta K_{1/2} = \frac{1}{2}\mathcal{M}_{\mathcal{K}}^{\langle\cdot\rangle}, \quad \mathcal{N}_{1/2} = \frac{1}{2}(K_{\max} + \mathcal{M}_{\mathcal{K}}^{\langle\cdot\rangle}). \tag{12}$$

These equations relate the NM measure proposed with the possibility of performing the task at hand, namely, the operation of a QV, under the assumption that the attacker attacks with

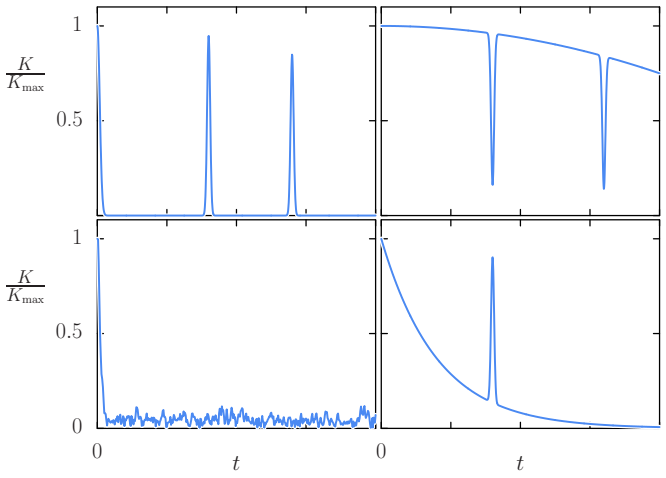

FIG. 1. Schematic examples of $K(t)/K_{\max}$ to be considered as QVs. Top left: Example with large δK_q and $\mathcal{M}^{(\cdot)}$, a good QV candidate. Top right: Worst-case scenario. Small δK_q, small (or null) $\mathcal{M}^{(\cdot)}$, and information always available for Eve to grab. Bottom left: Small $\mathcal{M}^{(\cdot)}$ and ΔK_q (poor for information retrieval) but decent $\mathcal{N}_q$ (good for information protection). Bottom left: A more general case, strongly depending on $\mathcal{M}^{(\cdot)}$ and the height of the peak at t_f.

probability 1/2. In particular, it gives an operational meaning to the measures proposed here and shows that, for the task proposed here, the figure of merit is $\mathcal{M}_{\mathcal{K}}^{(\cdot)}$.

In Fig. 1 we show some examples one could encounter for $K(t)/K_{\max}$. In the first one (top left) we have $\langle K(t)\rangle \approx 0$, $\mathcal{M}^{(\cdot)} \approx K(t_f)$, and

$$\Delta K_q \approx (1-q)\mathcal{M}^{(\cdot)}, \tag{13}$$

so for a fixed q, a large $\mathcal{M}^{(\cdot)}$ implies a high efficiency. This is in fact the ideal scenario for a QV, because most of the time the information is hidden and inaccessible to Eve and at time t_f the information can be retrieved with a high accuracy. If $\langle K(t)\rangle$ is very large, close to $K_{\max}$ (e.g., Fig. 1, top right), then, by definition, the channel is not a good QV: a large proportion of the information is readily available at all times before t_f. Here $K(t_f) < \langle K\rangle$ [so Eq. (11) does not hold], but the only possibility of having a good efficiency is the trivial $q \to 0$ case. If, on the other hand, $\langle K(t)\rangle$ and $K(t_f)$ are both very small (Fig. 1, bottom left)—again, $\mathcal{M}^{(\cdot)} \approx 0$—there is little chance of retrieving the information, even for small q, yielding a poor efficiency and $\mathcal{N}_q$. For large q, $\mathcal{N}_q \approx q K_{\max}$ can be large. The interpretation of this large value of $\mathcal{N}_q$ is that Eve will likely attack, but unsuccessfully. Finally, we consider the case where $K(t)$ decays monotonously except for one bump (e.g., Fig. 1, bottom right). The analysis now requires a little more care. If $K(t_f) < \langle K\rangle$, which happens for a small enough bump, then $\mathcal{M}_{\mathcal{K}}^{\cdot} = 0$, and there is no connection between ΔK_q (or $\mathcal{N}_q$) and $\mathcal{M}_{\mathcal{K}}^{\cdot}$. The analysis is similar to that in Fig. 1 (top right). On the other hand, if $\mathcal{M}^{(\cdot)} > 0$, the efficiency is bounded by Eq. (11), and for maximum $\mathcal{M}^{(\cdot)}$ the case is equivalent to the first one (top left).

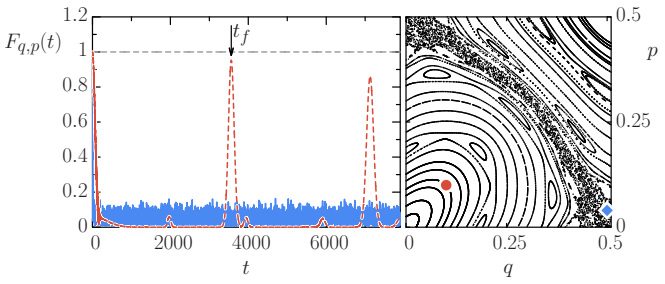

FIG. 2. Left: $F(t)$ as a function of time for two initial states of an environment modeled by the quantum Harper map. Right: Classical phase space of the environment for the parameters studied (see text). The two states of the environment in the left panel are coherent pure states centered at $(q,p) = (0.1,0.1)$—in the integrable region marked with a red circle, corresponding to the dashed (red) line in the left panel –, and $(q,p) = (0.5,0.04)$ – in the chaotic region, marked with a blue diamond, corresponding to the solid (blue) line in the left panel.

IV. EXAMPLES

In this section we present concrete physical examples of quantum channels where we can test the newly proposed measures and their relation to the QV scheme.

A. Environment with mixed dynamics

Let us discuss encoding quantum information in a qubit coupled to an environment in a dephasing manner. We consider that the environment evolves according to a dynamics that in the semiclassical limit is mixed, i.e., has integrable and chaotic regions in phase space.

A simple way to realize such an environment is to use a controlled kicked quantum map [32,33]. In this case, the environment evolution is slightly modified depending on the state of the qubit. This is equivalent to having a coupling with the environment that commutes with the Hamiltonians corresponding to the free evolution of each part, qubit, and environment.

Here we choose to use the quantum Harper map [34]. The evolution operator, in terms of the discrete conjugate space-momentum variables $\hat{q}$ and $\hat{p}$, is

$$U_k = \exp\left[-i\frac{k}{\hbar}\cos(2\pi\hat{p})\right]\exp\left[-i\frac{k}{\hbar}\cos(2\pi\hat{q})\right], \tag{14}$$

$\hbar \equiv 1/(2\pi N)$ being the effective Planck constant and N the dimension of the Hilbert space of the environment. The corresponding classical dynamics ($N \to \infty$) is given by

$$\begin{aligned} p_{n+1} &= p_n - k\sin(2\pi q_n), \\ q_{n+1} &= q_n + k\sin(2\pi p_{n+1}). \end{aligned} \tag{15}$$

The phase-space geometry is a 2-torus, so p_n and q_n are taken modulo 1. For $k = 0.2$, the dynamics is mixed (see Fig. 2). To use this closed system as an environment, we consider that the state of the qubit induces a small change in the parameter k of the map, so the evolution of the whole system for one time step is given by the Floquet operator

$$U = |0\rangle\langle 0|U_k + |1\rangle\langle 1|U_{k+\delta k} \tag{16}$$

and $U(t) = U^t$, for integer t. Throughout this example, we set $N = 4000$, $k = 0.2$, and $\delta k = 2\hbar$, unless otherwise stated. The initial state of the whole system is the uncorrelated state $\rho_{\rm sys} \otimes \rho_{{\rm env},q,p}$, where the environment is taken to be a pure coherent state centered in (q,p). The state of the qubit, obtained with unitary evolution in the whole system and partial tracing over the environment, is given by

$$\rho_{\rm sys}(t) = {\rm tr}_{\rm env}[U(t)\rho_{\rm sys} \otimes \rho_{{\rm env},q,p} U^\dagger(t)] = \Lambda_t^{q,p}(\rho_{\rm sys}). \quad (17)$$

In the basis of Pauli matrices $\{\sigma_i\} = \{\mathbb{I},\sigma_x,\sigma_y,\sigma_z\}/\sqrt{2}$, the induced channel takes the form

$$\Lambda_{q,p}(t) = \begin{pmatrix} 1 & 0 & 0 & 0 \\ 0 & {\rm Re}[f_{q,p}(t)] & {\rm Im}[f_{q,p}(t)] & 0 \\ 0 & {\rm Im}[f_{q,p}(t)] & {\rm Re}[f_{q,p}(t)] & 0 \\ 0 & 0 & 0 & 1 \end{pmatrix}, \quad (18)$$

where

$$f_{q,p}(t) = {\rm tr}[\rho_{{\rm env},q,p} U_{k+\delta k}(t)^\dagger U_k(t)] \quad (19)$$

is the expectation value of the echo operator $U_{k+\delta k}(t)^\dagger U_k(t)$ with respect to the corresponding coherent state (also known as the fidelity amplitude). We also define the fidelity, $F_{q,p}(t) = |f_{q,p}(t)|$, for later convenience. Note that the channel depends, up to unitary operations, only on $F_{q,p}(t)$, and thus all capacities will be functions solely of this quantity. In Fig. 2 (left) we show two examples of $F_{q,p}(t)$, for different initial conditions of the environment (marked by large symbols in Fig. 2, right). One can see that in the case where the environment starts inside the chaotic sea (blue diamond), the system has very small $\mathcal{M}_F^{(\cdot)}$ and $\mathcal{M}_F^{\rm max}$ values, and therefore from Eq. (12) it will be a very bad QV.

An interesting point in Fig. 2 is how $\mathcal{M}_F^{(\cdot)}$ and $\mathcal{M}_F^{\rm max}$ compare to $\mathcal{M}^{\rm BLP}$ and $\mathcal{M}^{\rm RHP}$.

In terms of $F_{q,p}(t)$ the latter are given by

$$\begin{aligned} \mathcal{M}^{\rm BLP} &= \int_{0,\dot{F}>0}^{t_{\rm cut}} d\tau \dot{F}_{q,p}(\tau), \\ \mathcal{M}^{\rm RHP} &= \int_{0,\dot{F}>0}^{t_{\rm cut}} d\tau \frac{\dot{F}_{q,p}(\tau)}{F_{q,p}(\tau)}, \end{aligned} \quad (20)$$

where $t_{\rm cut}$ indicates the cutoff time. The $[F_{q,p}(\tau)]^{-1}$ term in $\mathcal{M}^{\rm RHP}$ can be problematic when $F_{q,p}(\tau)$ is very small, which is exactly the case for an initial state located in the chaotic region. In Table I the values of all four measures, based on F, corresponding to Fig. 2 are listed. The values reported in the table highlight important characteristics of all four measures. On the one hand, for non-monotonicity-based measures, intuitively we expect that a fast-decaying $K(t)$ followed by sharp and high revivals would yield a larger value of NM. This is not the case for $\mathcal{M}^{\rm BLP}$ and $\mathcal{M}^{\rm RHP}$ (at least in this particular example), for different reasons. In the case of $\mathcal{M}^{\rm RHP}$ it is due to the small denominator and in the case of $\mathcal{M}^{\rm BLP}$ it is due to fluctuations (and finite N). These facts are further illustrated in the color density plots in Fig. 3. We see that in all cases the underlying classical structure is clearly outlined. For both $\mathcal{M}_F^{(\cdot)}$ and $\mathcal{M}_F^{\rm max}$ an additional structure appears that resembles the unstable manifolds. The measures $\mathcal{M}_F^{(\cdot)}$, $\mathcal{M}_F^{\rm max}$, and $\mathcal{M}^{\rm BLP}$ all seem to peak in the vicinity of the border between chaotic and regular behavior. As stated before, the $\mathcal{M}^{\rm RHP}$ measure behaves differently, as it is larger in the chaotic region.

TABLE I. Comparison between different values of measures of non-Markovianity (NM) for the two situations depicted in Fig. 2. We cut the integral in Eq. (20) at $t = 8000$. The inherent fluctuations present for this finite-dimensional environment cause the integrable situation (with larger fluctuations) to reach larger values for the NM measures $\mathcal{M}^{\rm BLP}$ and $\mathcal{M}^{\rm RHP}$ than does the chaotic counterpart. On the other hand, both $\mathcal{M}_F^{(\cdot)}$ and $\mathcal{M}_F^{\rm max}$ capture well the idea of the QV, reporting large values for the integrable case and small values for the chaotic one.

In Fig. 2	$\mathcal{M}_F^{(\cdot)}$	$\mathcal{M}_F^{\rm max}$	$\mathcal{M}^{\rm BLP}$	$\mathcal{M}^{\rm RHP}$
Filled red circle	0.899	0.953	3.3	1333.97
Filled blue diamond	0.108	0.194	62.92	6274.89

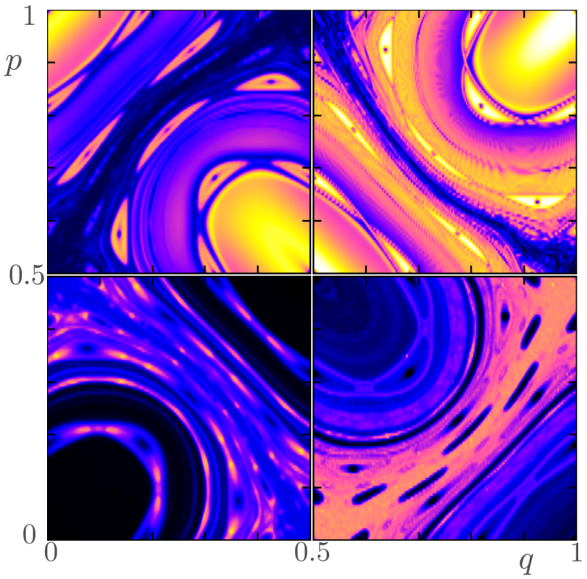

FIG. 3. Mapping of the classical phase space obtained from the different non-Markovianity measures discussed, for the quantum Harper map with $N = 8000$, $K = 0.2$, $\delta K/\hbar = 2$, and maximum time $t_{\rm cut} = 16\,000$. The color code is dark/black = 0, light/white = max. The different panels correspond to $\mathcal{M}_F^{(\cdot)}$ with a maximum value of the measure of 1 (top left), $\mathcal{M}_F^{\rm max}$ with a maximum value of 1 (top right), $\mathcal{M}^{\rm BLP}$ with a maximum value of 200 (bottom left), and $\mathcal{M}^{\rm RHP}$ with a maximum value of 19 000 (bottom right).

Note that the measure $M_F^{(\cdot)}$ can be associated with the task of transmitting classical information (without the use of entanglement) encoded initially in the states $|\pm\rangle$.

B. Non-Markovian Jaynes-Cummings model

In order to explore and compare the different measures of NM discussed throughout this work, we now consider the paradigmatic JCM [28], which has served as a testbed in quantum optics (see, e.g., [1]). In this model, a two-level atom is coupled to a bosonic bath, which induces a degradable channel in the qubit. We take advantage of the fact that a lot is known about this model analytically and we build upon known results.

The Hamiltonian of the system is $H = H_0 + H_I$, where H_0 is the free Hamiltonian of the atom plus the reservoir and H_I the interaction between them. In particular, $H_0 = \omega_0\sigma_+\sigma_- + \sum_k \omega_k b_k^\dagger b_k$, where $\sigma_\pm$ are the rising and lowering operators in the atom, ω_0 is the energy difference between the two levels in the atom, b_k and $b_k^\dagger$ are the creation and annihilation operators of mode k of the bath, and ω_k is its frequency. The interaction Hamiltonian is given by $H_I = \sigma_+ \otimes B + \sigma_- \otimes B^\dagger$, with $B = \sum_k g_k b_k$ and g_k the coupling of the qubit to mode k. In the limit of an infinite number of reservoir oscillators and a smooth spectral density, this model leads to the channel [1]

$$\Lambda_t[\rho] = \begin{pmatrix} 1-|G(t)|^2\rho_{ee} & G(t)\rho_{ge} \\ G^*(t)\rho_{ge}^* & |G(t)|^2\rho_{ee} \end{pmatrix}, \tag{21}$$

where the initial state is $\rho = \left(\begin{smallmatrix} 1-\rho_{ee} & \rho_{ge} \\ \rho_{ge}^* & \rho_{ee} \end{smallmatrix}\right)$.

The function $G(t)$ is the solution to the equation $\dot{G}(t) = -\int_0^t d\tau f(t-\tau)G(\tau)$, with $G(0) = 1$, and $f(t-\tau)$ is the two-point correlation function of the reservoir. For a Lorenzian spectral density

$$f(t) = \tfrac{1}{2}\gamma_0\lambda e^{-|t|(\lambda - i\delta)}, \tag{22}$$

we find

$$G(t) = e^{-\frac{1}{2}t(\lambda-i\delta)}\left[\frac{(\lambda - i\delta)}{\Omega}\sinh\left(\frac{\Omega t}{2}\right) + \cosh\left(\frac{\Omega t}{2}\right)\right], \tag{23}$$

where $\Omega = \sqrt{-2\gamma\lambda + (\lambda - i\delta)^2}$. Here, γ_0 is the strength of the system-reservoir coupling, λ is the spectral width, and δ is the detuning between the peak frequency of the spectral density and the transition frequency of the atom [35].

In what follows, we study the NM measures $\mathcal{M}_\mathcal{K}^\infty$, $\mathcal{M}_\mathcal{K}^{\max}$, and $\mathcal{M}_\mathcal{K}^{(\cdot)}$ for the capacities $\mathcal{Q}$ (quantum capacity), $\mathcal{C}$ (entanglement-assisted classical capacity), and $\mathcal{D}$ (distinguishability of the states $|\pm\rangle$). The quantum capacity is defined as the maximal amount of quantum information (per channel use, measured as the number of qubits) that can be reliably transmitted through the channel. It is given explicitly in terms of the maximization [36] $\max_{p\in[0,1]}\{H_2(|G(t)|^2 p) - H_2((1-|G(t)|^2)p)\}$ for $|G(t)|^2 > 1/2$ and 0 for $|G(t)|^2 \leqslant 1/2$. The entanglement-assisted classical capacity $\mathcal{C}$ is defined as the maximal amount of classical information (per channel use; measured as the number of classical bits) that can be reliably transmitted through the channel when Alice and Bob are allowed to use an arbitrary number of shared entangled states [31]. For the present channel it is given by [36] $\mathcal{C} = \max_{p\in[0,1]}\{H_2(p) + H_2(|G(t)|^2 p) - H_2((1-|G(t)|^2)p)\}$. Finally, we also consider the BLP measure defined in Eq. (4). In this case the initial states which maximize the various types of NM measures may be chosen invariably as the two eigenstates of the Pauli matrix σ_x [10]. Thereby, we obtain $K(t) = |G(t)|$.

Figure 4 shows a comparison between the measures $\mathcal{M}_\mathcal{K}^{(\cdot)}$ and $\mathcal{M}_\mathcal{K}^{\max}$, introduced in this work, and their counterpart $\mathcal{M}_\mathcal{K}^\infty$. The measures regarding the average $\mathcal{M}_\mathcal{K}^{(\cdot)}$ are notoriously smaller than the measures regarding both the maximum revival and the integrated revivals. In fact, we find that $\mathcal{M}_\mathcal{K}^{(\cdot)} \leqslant \mathcal{M}_\mathcal{K}^{\max}$, in agreement with (7), and $\mathcal{M}_\mathcal{K}^{\max} \leqslant \mathcal{M}_\mathcal{K}^\infty$. The measures related to the BLP criterion (dotted lines) behave similarly in all three cases, decaying monotonously with δ/λ. In the case of the entanglement-assisted classical capacity, $\mathcal{M}_\mathcal{C}^\infty$ and $\mathcal{M}_\mathcal{C}^{\max}$

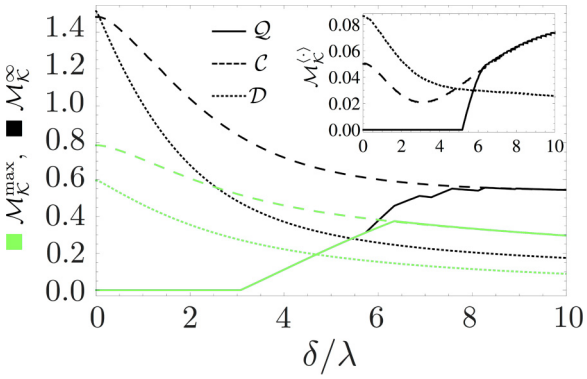

FIG. 4. Comparative results of the measures of quantum non-Markovianity treated in this work for the Jaynes-Cummings model, as a function of the scaled detuning δ/λ, with a coupling of $\gamma = 20\lambda$. We show three types of measures—$\mathcal{M}_\mathcal{K}^\infty$ (black lines), $\mathcal{M}_\mathcal{K}^{\max}$ (green lines), and $\mathcal{M}_\mathcal{K}^{(\cdot)}$ (inset)—for three capacities: the quantum capacity $\mathcal{Q}$ (solid lines), classical entanglement-assisted capacity $\mathcal{C}$ (dashed lines), and capacity based on the distinguishability $\mathcal{D}$ (dotted lines).

also decay monotonously. However, $\mathcal{M}_\mathcal{C}^{(\cdot)}$ has a minimum at $\delta/\lambda \approx 3$. Beyond that point $\mathcal{M}_\mathcal{C}^{(\cdot)}$ increases a bit further but, finally, decays to 0. In this region, $\mathcal{M}_\mathcal{C}^{(\cdot)} = \mathcal{M}_\mathcal{Q}^{(\cdot)}$, which is shown in Fig. 4. The measures related to the quantum capacity (solid lines) show the most complicated behavior. $\mathcal{M}_\mathcal{Q}^\infty$ and $\mathcal{M}_\mathcal{Q}^{\max}$ are equal to 0 until $\delta/\lambda \approx 3$, $\mathcal{M}_\mathcal{Q}^{(\cdot)}$ is equal to 0 until $\delta/\lambda \approx 5$. Beyond these points, the measures increase linearly. From $\delta/\lambda \approx 6.5$ on, $\mathcal{M}_\mathcal{Q}^{\max}$ and $\mathcal{M}_\mathcal{Q}^{(\cdot)}$ reach the corresponding curves for the classical capacity. For somewhat larger values of δ/λ this also happens for $\mathcal{M}_\mathcal{Q}^\infty$.

The fact that for quantum capacities, $\mathcal{M}_\mathcal{Q}^\infty$ and $\mathcal{M}_\mathcal{Q}^{\max}$ start to deviate from 0 at the same point, $\delta/\lambda \approx 3$, illustrates Eq. (8). Other interesting features that can be appreciated in $\mathcal{M}_\mathcal{Q}^\infty$ are the multiple discontinuities in the derivative with respect to the detuning. This is due to the sudden appearance of new bumps in the quantum capacity of the channel, to which this measure is sensitive. Moreover, for most instances of $\mathcal{K}$, $\mathcal{M}_\mathcal{K}^\infty$ can be discontinuous in the space of finite quantum processes, if we consider the maximum-norm, so the measures are not stable

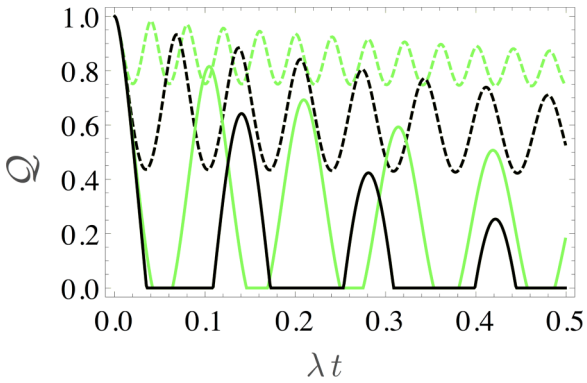

FIG. 5. Quantum capacities of the non-Markovian Jaynes-Cummings model with a strong coupling, $\gamma/\lambda = 1000$. Solid curves correspond to $\delta/\lambda = 0$ (black) and $\delta/\lambda = 40$ (green); dashed curves, to $\delta/\lambda = 80$ (black) and $\delta/\lambda = 150$ (green).

TABLE II. Measures treated in this work of the quantum capacities shown in Fig. 5, with $t_{\text{cut}} = \infty$.

In Fig. 5	δ/λ	$\mathcal{M}_{\mathcal{Q}}^{\langle\cdot\rangle}$	$\mathcal{M}_{\mathcal{Q}}^{\max}$	$\mathcal{M}_{\mathcal{Q}}^{\infty}$
Solid black line	0	0.4072	0.6419	1.4322
Solid green line	40	0.4301	0.8154	4.4928
Dashed black line	80	0.2564	0.4963	6.0953
Dashed green line	150	0.1210	0.2309	4.7588

with respect to small deviations in the quantum dynamics. In particular, low-amplitude high-frequency noise can make $\mathcal{M}_{\mathcal{K}}^{\infty}$ increase arbitrarily, whereas it has a small effect (proportional to the amplitude) in the case of $\mathcal{M}_{\mathcal{K}}^{\langle\cdot\rangle}$ and $\mathcal{M}_{\mathcal{K}}^{\max}$.

Regarding the classical capacity, it is noteworthy that the different cases do not share the same tendency; $\mathcal{M}_{\mathcal{C}}^{\max}$ and $\mathcal{M}_{\mathcal{C}}^{\infty}$ diminish with the detuning (as opposed to the quantum capacity cases), but $\mathcal{M}_{\mathcal{C}}^{\langle\cdot\rangle}$ shows a nonmonotonic behavior, mimicking fidelity until $\delta/\lambda \approx 3$ and then resembling the quantum capacity. A direct consequence of the fact that $\mathcal{Q} \leqslant \mathcal{C}$ is that $\mathcal{M}_{\mathcal{Q}}^{\cdot} \leqslant \mathcal{M}_{\mathcal{C}}^{\cdot}$, as can be seen from the fact that, for all colors in Fig. 4, the dashed line bounds the solid line (here, the dot denotes any of max , $\langle\cdot\rangle$, or ∞). As a general remark, we also observe that $\mathcal{M}_{\mathcal{K}}^{\langle\cdot\rangle}$ is much smaller than $\mathcal{M}_{\mathcal{K}}^{\max}$ and $\mathcal{M}_{\mathcal{K}}^{\infty}$. This is due to the fact that the peaks in the different capacities are thick, and the system, in fact, would not serve as a good QV.

Figure 5 shows the evolution of several quantum capacities for the JCM varying the detuning while keeping the reservoir coupling fixed. Table II lists the values of the corresponding measures of NM treated in this work. It shows that large detunings lead to poor scenarios for a QV operation, while for 0 and small detuning there are better situations for use of the QV. The time when the first peak in the capacity appears can be tuned by choosing the correlation time of the bath. Figure 6 shows a density plot of the NM measure, $\mathcal{M}_{\mathcal{Q}}^{\langle\cdot\rangle}$, as a function of the channel parameters, δ and γ. It shows how a region of high $\mathcal{M}_{\mathcal{Q}}^{\langle\cdot\rangle}$ appears as the coupling increases, as long as the detuning is not too strong ($\sim$10). This is because large couplings induce a rapid decay in the quantum capacity, while oscillations from the detuning restore the capacity. For large detunings, the probability of transitions in the atom is low, which implies that the capacity initially has small oscillations close to 1 with a slow decay. For small couplings $\gamma/\lambda < 1/2$ and zero detuning, the capacity decays monotonically [23]; this makes all the measures discussed equal to 0 and therefore a useless QV.

V. CONCLUSIONS

In the light of the considerable advances in the experimental manipulation of quantum systems at the very fundamental level, understanding and controlling how a quantum system interacts with its surroundings is of paramount importance.

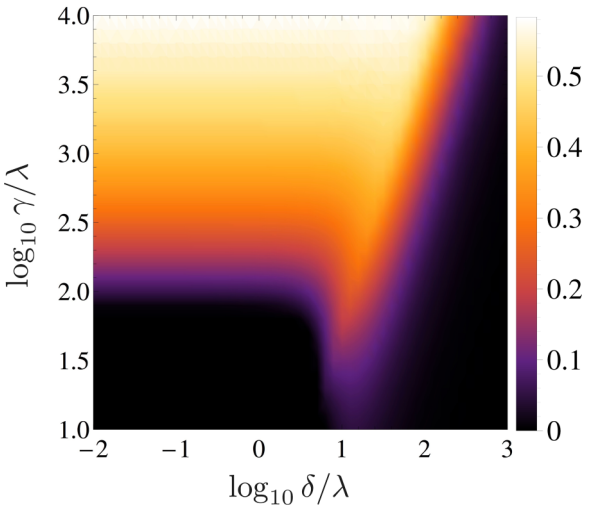

FIG. 6. Density plot of $\mathcal{M}_{\mathcal{Q}}^{\langle\cdot\rangle}$ for the non-Markovian Jaynes-Cummings model as a function of its parameters.

In this context, finite, structure-rich environments play an important role, and the challenge has been to understand and control the resulting non-Markovian evolution.. In particular, one might wonder whether there is a possibility of taking advantage of the flow of information back to the system which is characteristic of NM. Defining and quantifying NM is a nontrivial task. In this work we have shown that one can define and quantify non-Markovian behavior in a physically meaningful way: one that is insightful and avoids the drawbacks of previous attempts, such as divergence in very generic cases and counterintuitive outcomes. Moreover, we could define the new measure with a task in mind: hiding and retrieving classical or quantum information using a quantum channel. The efficiency with which this task is accomplished is directly related to the NM measure. Finally, we have illustrated the proposed measures with simple physical examples. Several important issues are yet to be addressed. For example, an important point is the relation between the notion quantum NM and its classical counterpart. This relation is far from straightforward as pointed out in previous work [37]. Some advances in this direction were proposed recently in [38].

ACKNOWLEDGMENTS

We acknowledge support from UNAM-PAPIIT Grant No. IN111015 and CONACyT Grants No. 153190 and No. 129309, as well as useful discussions with Sabrina Maniscalco and Heinz-Peter Breuer. I.G.M. and D.A.W. received support from ANPCyT (Grant No. PICT 2010-1556), UBACyT, and CONICET (Grants No. PIP 114-20110100048 and No. PIP 11220080100728). I.G.M. and C.P. shared a binational grant from CONICET (Grant No. MX/12/02 Argentina) and CONACYT (México).

[1] H. Breuer and F. Petruccione, *The Theory of Open Quantum Systems* (Oxford University Press, Oxford, UK, 2007).

[2] M. A. Schlosshauer, *Decoherence and the Quantum-to-Classical Transition* (Springer, Berlin, 2007).

[3] J. M. Raimond, M. Brune, and S. Haroche, Rev. Mod. Phys. **73**, 565 (2001).

[4] D. Leibfried, R. Blatt, C. Monroe, and D. Wineland, Rev. Mod. Phys. **75**, 281 (2003).

[5] I. Bloch, J. Dalibard, and W. Zwerger, Rev. Mod. Phys. **80**, 885 (2008).

[6] J. L. O'Brien, A. Furusawa, and J. Vučković, Nat. Photon. **3**, 687 (2009).

[7] T. D. Ladd, F. Jelezko, R. Laflamme, Y. Nakamura, C. Monroe, and J. L. O'Brien, Nature **464**, 45 (2010).

[8] G. Lindblad, Commun. Math. Phys. **48**, 119 (1976).

[9] V. Gorini, A. Kossakowski, and E. C. G. Sudarshan, J. Math. Phys. **17**, 821 (1976).

[10] H.-P. Breuer, J. Phys. B: At. Mol. Opt. Phys. **45**, 154001 (2012).

[11] A. Rivas, S. F. Huelga, and M. B. Plenio, Rep. Prog. Phys. **77**, 094001 (2014).

[12] H.-P. Breuer, E.-M. Laine, J. Piilo, and B. Vacchini, arXiv:1505.01385.

[13] S. F. Huelga, A. Rivas, and M. B. Plenio, Phys. Rev. Lett. **108**, 160402 (2012).

[14] C. Cormick, A. Bermudez, S. F. Huelga, and M. B. Plenio, New J. Phys. **15**, 073027 (2013).

[15] D. M. Reich, N. Katz, and C. P. Koch, Scientific Reports **5**, 12430 (2015).

[16] S. Deffner and E. Lutz, Phys. Rev. Lett. **111**, 010402 (2013).

[17] H.-P. Breuer, E.-M. Laine, and J. Piilo, Phys. Rev. Lett. **103**, 210401 (2009).

[18] A. Rivas, S. F. Huelga, and M. B. Plenio, Phys. Rev. Lett. **105**, 050403 (2010).

[19] X.-M. Lu, X. Wang, and C. P. Sun, Phys. Rev. A **82**, 042103 (2010).

[20] R. Vasile, S. Maniscalco, M. G. A. Paris, H.-P. Breuer, and J. Piilo, Phys. Rev. A **84**, 052118 (2011).

[21] S. Luo, S. Fu, and H. Song, Phys. Rev. A **86**, 044101 (2012).

[22] S. Lorenzo, F. Plastina, and M. Paternostro, Phys. Rev. A **88**, 020102 (2013).

[23] B. Bylicka, D. Chruściński, and Maniscalco, Sci. Rep. **4**, 5720 (2014).

[24] M. Žnidarič, C. Pineda, and I. García-Mata, Phys. Rev. Lett. **107**, 080404 (2011).

[25] D. P. Divincenzo, D. W. Leung, and B. M. Terhal, IEEE Trans. Info. Theory **48**, 580 (2002).

[26] D. DiVincenzo, P. Hayden, and B. Terhal, Found. Phys. **33**, 1629 (2003).

[27] W. Matthews, S. Wehner, and A. Winter, Commun. Math. Phys. **291**, 813 (2009).

[28] E. T. Jaynes and F. W. Cummings, Proc. IEEE **51**, 89 (1963).

[29] I. Bengtsson and K. Zyczkowski, *Geometry of Quantum States: An Introduction to Quantum Entanglement* (Cambridge University Press, Cambridge, UK, 2006).

[30] T. Heinosaari and M. Ziman, *The Mathematical Language of Quantum Theory: From Uncertainty to Entanglement* (Cambridge University Press, Cambridge, UK, 2012).

[31] G. Smith, in *IEEE Information Theory Workshop (ITW), 2010* (IEEE, Piscataway, NJ, 2010), pp. 1–5.

[32] I. García-Mata, C. Pineda, and D. Wisniacki, Phys. Rev. A **86**, 022114 (2012).

[33] I. García-Mata, C. Pineda, and D. A. Wisniacki, J. Phys. A: Math. Theor. **47**, 115301 (2014).

[34] P. Leboeuf, J. Kurchan, M. Feingold, and D. P. Arovas, Phys. Rev. Lett. **65**, 3076 (1990).

[35] The case without detuning is treated in detail in [1]; the present case with detuning was first solved in Ref. [23], but with a minor mistake. Here, we present the corrected expression.

[36] V. Giovannetti and R. Fazio, Phys. Rev. A **71**, 032314 (2005).

[37] B. Vacchini, A. Smirne, E.-M. Laine, J. Piilo, and H.-P. Breuer, New J. Phys. **13**, 093004 (2011).

[38] S. Wißmann, B. Vacchini, and H.-P. Breuer, Phys. Rev. A **92**, 042108 (2015).